International Journal of Technology 10(6): 1235-1242
ISSN 2086-9614

EFFECT OF NaCl ADDITION ON NANO ROSETTE TiO_2 CRYSTAL GROWTH DURING HYDROTHERMAL DEPOSITION

Nofrijon Sofyan[1*], Aga Ridhova[2], Marshall C. Sianturi[1], Akhmad Herman Yuwono[1]

[1]*Department of Metallurgical and Materials Engineering, Faculty of Engineering, Universitas Indonesia, Kampus UI Depok, Depok 16424, Indonesia*
[2]*Research Center for Metallurgy and Materials, Indonesian Institute of Sciences, Tangerang Selatan, Banten 15314, Indonesia*

(Received: August 2019 / Revised: October 2019 / Accepted: October 2019)

ABSTRACT

The effect of NaCl on the crystal growth of nano rosette TiO_2 hydrothermally grown on a glass substrate was examined. Nano rosette TiO_2 was synthesized through deposition on a glass substrate via hydrothermal reaction at 170°C for 6 hours. The effect of NaCl on nano rosette TiO_2 crystal growth during the hydrothermal process was observed through the addition of concentrations of 0, 2.5, 5, and 10% v/v NaCl to the mixture of the precursors. Formation and growth of the crystal were characterized using X-ray diffraction, whereas morphology was examined using a scanning electron microscope. X-ray diffractograms revealed that the crystal belonged to rutile $P4_2/mnm$ with lattice parameters of a = 4.557(6) Å and c = 2.940(5) Å. Morphology of the reaction product showed that the addition of NaCl inhibited the crystal growth of nano rosette TiO_2 with an average rosette petal cross-sectional size 80% smaller than that of the crystal grown with no NaCl addition.

Keywords: Hydrothermal; Nano rosette; Nanoscale; Sodium chloride; Titanium dioxide

1. INTRODUCTION

In current advanced materials development, nanomaterials are attracting the attention of many researchers due to inherent properties resulting from the physicochemical changes of a substance at nanoscale. Nanoscale building blocks, specifically in the forms of 3D architectures of hierarchical nanostructures such as nanowires (Zhu et al., 2018), nanorods (Govindaraj et al., 2017), nanosheets (Zhong et al., 2015) and nanoflowers (Ma et al., 2017), have become the focus, receiving closer attention due to their unique properties and promising applications in many areas (Banfield & Veblen, 1992).

For a long time, Titanium dioxide or TiO_2 has been the subject of intensive research because of its unique properties with promising application in numerous areas. Titanium dioxide is also known for its polymorphic characteristic, in which it may have several crystal structures, including brookite, anatase, and rutile crystal structures (Khan et al., 2017). Due to these unique properties, not only has it been used tremendously in conventional applications such as white pigment in paint, food coloring, and personal care products (Bai & Zhou, 2014), but it has also been used as advanced materials for sensors (Nakata & Fujishima, 2012), photocatalysts (Xie et al., 2009; Liang et al., 2017; Longoni et al., 2017; Rahman et al., 2018), dye-sensitized solar cells (Sofyan et al., 2017; Sofyan et al., 2019), perovskite solar cells (Dahl et al., 2014), and

*Corresponding author's email: nofrijon.sofyan@ui.ac.id, Tel. + 62-21-7863510, Fax. +62-21-7872350
Permalink/DOI: https://dx.doi.org/10.14716/ijtech.v10i6.3630

batteries (Saif et al., 2012).

The use of 3D nanostructures TiO_2 in the form of hierarchical flower-like TiO_2 nanostructures has recently increased due to their excellent optical, electrical, and electronic properties with promising use in many applications (Bu et al., 2015; Zhang et al., 2018). As a result, many investigators have put their efforts into improving methods in synthesizing 3D flower-like nanostructure TiO_2. For example, TiO_2 with 3D nano-flower hierarchical structures has been proven to enhance its photocatalytic property (Zhou et al., 2013; Bu et al., 2015). In separate work, Xiao et al. (2017) and Govindasamy et al. (2016) have reported that the use of a combination of TiO_2 compact layers with the growth of TiO_2 nanorods as an electron transporting layer has improved the performance of perovskite solar cells.

Despite its promising use in many applications, there are still many problems in synthesizing flower-like structure TiO_2, such as homogeneity and coverage area, in the case of the deposition process. There are also very few references that discuss the direct synthesis of rutile TiO_2 with high homogeneity, especially in the form of rutile nano rosette TiO_2. Another problem comes from the fact that, if the deposition can have a high coverage area and be homogeneous, the crystal might grow uncontrolled and thus result in quite large crystal size. Because of this, during the process, growth needs to be controlled.

In this work, 3D hierarchical nano rosette TiO_2 has been grown via a hydrothermal process on a glass substrate with enhanced homogeneity and coverage area, whilst at the same time offering a controllable crystal growth during the synthesis, resulting in a controlled size of nano rosette TiO_2. The characteristics of the nano rosette TiO_2 from the reaction products in different controlled environments using sodium chloride (NaCl) at different concentrations on crystal formation and growth during the hydrothermal deposition are presented and discussed.

2. METHODS

2.1. Materials

The raw materials were titanium (IV) isopropoxide (TTIP, ≥ 97.0% Sigma-Aldrich), NaCl saturated solution (Sigma-Aldrich), and hydrochloric acid (HCl 37%, Merck). For the solvents, acetone, ethanol, and distilled water were used throughout the experiment, except where stated otherwise. For the substrate, a fluorine-doped tin oxide (FTO, 30 Ω/cm^2) glass substrate was used.

2.2. Preparation of Nano Rosette TiO_2

Nano rosette TiO_2 was prepared via a hydrothermal method as described in Govindasamy et al. (2016) and Xiao et al. (2017), with slight modification (Sofyan et al., 2018), explained as follows. Different concentrations of 0%, 1%, 2.5%, 5% and 10% v/v NaCl saturated solution were added into a fix mixture of 1:1 of distilled water and HCl to reach a total volume of 40 mL. The mixture was ultrasonicated under an ambient condition for 5 minutes before being added with 450 μL TTIP. The mixture was continued under ultrasonication for another 5 minutes until a clear solution was obtained. At the same time, the glass substrate was prepared by cleaning it in a mixed solution of distilled water, acetone, and ethanol with a volume ratio of 1:1:1 in an ultrasonicator for 10 minutes. The cleaned substrate was then placed horizontally at the bottom of a 100 mL Teflon-lined stainless-steel autoclave before being poured with the previously prepared solution containing TTIP. The hydrothermal synthesis was conducted at 170°C for an optimized time of 6 hours (Sofyan et al., 2018) in a vacuum oven (DZF-6050, Berkeley Scientific). After the synthesis, the autoclave was cooled to room temperature under flowing water for approximately 5 minutes. The glass substrate was then taken out of the autoclave, rinsed with distilled water, and allowed to dry in air for 15 minutes before being calcined on a hotplate (Cimarec SP 131320-33, Thermo Scientific) at 450°C for 30 minutes and ready for characterization.

2.3. Characterization

The characterization was performed under an ambient condition with no control on humidity nor pressure. The morphology of the reaction product was examined through secondary electron images obtained using field emission scanning electron microscope (FE-SEM, FEI Inspect F50) and high resolution transmission electron microscope (HRTEM, FEI Tecnai G2 S-Twin), whereas the structural characteristics of the sample were observed using X-ray diffraction (XRD, PANalytical X'Pert PRO) operating at 40 kV 30 mA with Cu Kα radiation (λ = 1.5406 Å).

3. RESULTS AND DISCUSSION

The structural formation of nano rosette TiO_2 via hydrothermal reaction at different NaCl additions was characterized using X-ray diffraction, whereas the morphological characteristics on the crystal growth was performed through secondary electron images obtained using FESEM. The structural characteristics, crystallinity, and the phase formed at different NaCl variations examined using XRD technique are given in Figure 1. As can be observed from the X-ray diffractograms, each sample at 0%, 2.5%, 5%, and 10% v/v NaCl addition showed the phase formation of a crystalline structure but with different crystallinity.

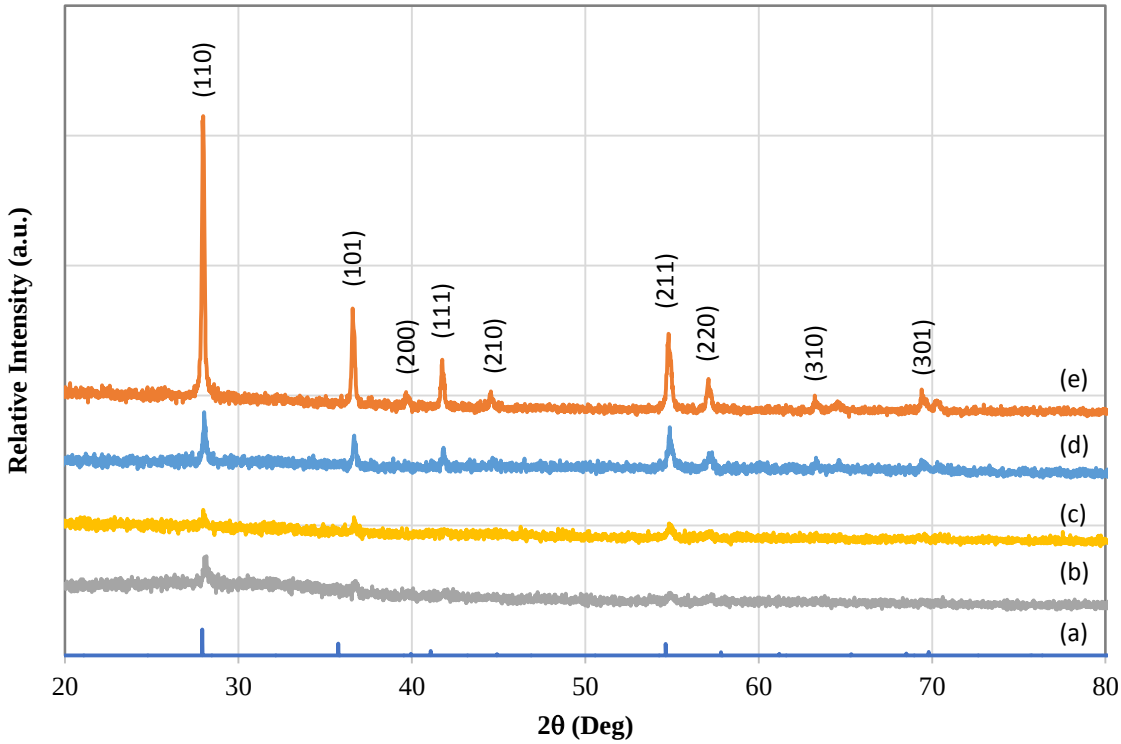

Figure 1 X-ray diffractograms of: (a) rutile TiO_2 reference (JPDS 01-082-0154); and nano rosette TiO_2 grown hydrothermally with the addition of (b) 2.5%; (c) 5%; (d) 10%; and (e) 0% v/v NaCl

All peaks have been identified and show the same trend and are confirmed to be rutile crystal structure TiO_2 with a reference JCPDS file No. 01-082-0514 indexed to tetragonal $P4_2/mnm$. Some peaks, however, shift to high angles due to differences in lattice parameters. No other characteristic peaks of other phases and or impurities are detected in the diffractograms. For the sample with no NaCl addition (0% v/v NaCl), there are four distinct diffraction peaks observed, at 2θ 27.659°, 36.579°, 41.742°, and 54.776°, corresponding to (110), (101), (111), and (211) of rutile TiO_2 crystal planes, respectively. Calculation showed that lattice parameters of *a* 4.557(6) Å and *c* is 2.940(5) Å. The average crystallite size has also been calculated using the Scherrer formula (Patterson, 1939), with an average crystallite size of 77 nm (Sofyan et al., 2018). This

finding is also supported with the results obtained using high resolution transmission electron microscope (HRTEM), as can be seen in Figure 2.

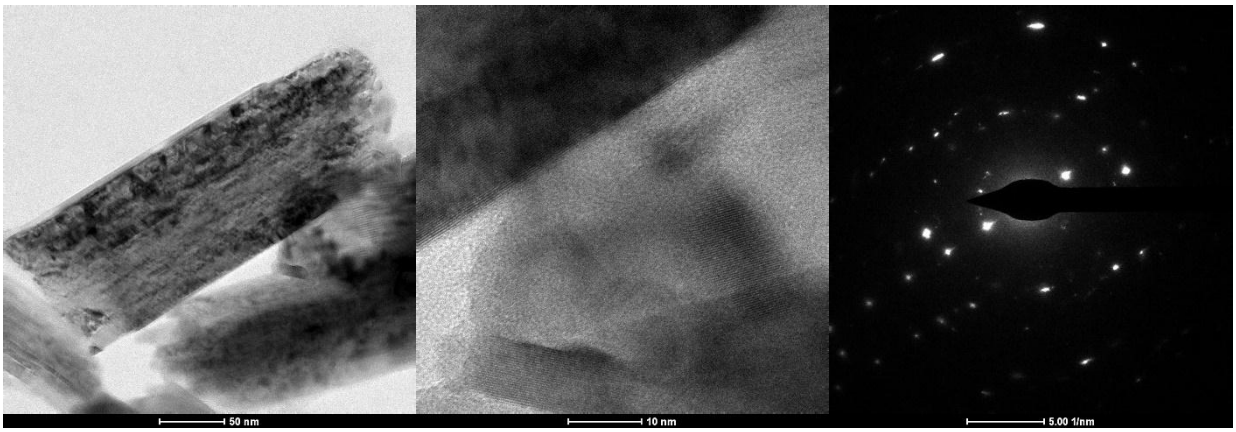

(a) (b) (c)

Figure 2 High resolution transmission electron images (HRTEM) of nano rosette TiO_2 hydrothermally synthesized at 170°C for 6 hours with no addition of NaCl: (a) at low magnification (bar scale 50 nm); (b) at high magnification (bar scale 5 nm); and (c) the corresponding selected area diffraction pattern

For the sample with NaCl addition, different crystallinity was observed through the intensity. Nonetheless, the diffractograms show at least three major diffraction peaks, observed at 2θ 28°, 36.6°, and 54.8° corresponding to the rutile TiO_2 crystal planes of (110), (101), and (211), respectively. Compared to the diffraction intensity without the addition of NaCl (Figure 1e), the diffraction pattern of the sample with the addition of NaCl shows a sharp decrease in intensity for 2.5% v/v NaCl. This decrease is expected to be due to the difference in the crystallinity of the nano rosette TiO_2. The addition of 2.5% v/v NaCl suffices to abruptly hinder crystal growth during the hydrothermal reaction. However, it seems that higher NaCl concentration in the mixture will promote crystal growth, and the diffraction peaks gain their intensity again. In this instance, it is expected that the addition of NaCl decreases the crystallinity of the nano rosette TiO_2 because of the inhibition by sodium ion of the crystal growth during hydrothermal reaction and thus makes the rosette petal size smaller than that of without the addition of NaCl. With more NaCl, there would be more competing ions; however, the exact reason is yet to be confirmed.

The morphological characteristics of the reaction products at various NaCl concentrations were examined through secondary electron images obtained using FESEM, and the results are given in Figure 3. As can be observed, there is a significant difference in the size of crystals' rosette petals with and without the addition of NaCl. Without the addition of NaCl, the crystal has a tendency to grow larger than that of with the addition of NaCl. The rosette petal size at 0% v/v NaCl is about 200–250 nm (Figure 3a). With the addition of 2.5% v/v NaCl, the rosette petal size decreases to about 50 nm (Figure 3b), whereas with the addition of 5% v/v NaCl, the rosette petal is about 80 nm (Figure 3c). The rosette petal gains in growth again with the addition of 10% v/v NaCl, in which the rosette petal grows to about 100 nm (Figure 3d). Taking the smallest petal size of about 50 nm with the addition of 2.5% v/v NaCl, the reduction of nano rosette TiO_2 petal size from the one without NaCl addition (250 nm) is of about 80%. This result is in agreement with the results obtained from the XRD results. Other investigators have found that the addition 8% of saturated sodium chloride into a growth solution could reduce nanorod TiO_2 diameter to about 39% (Liu & Aydil, 2009).

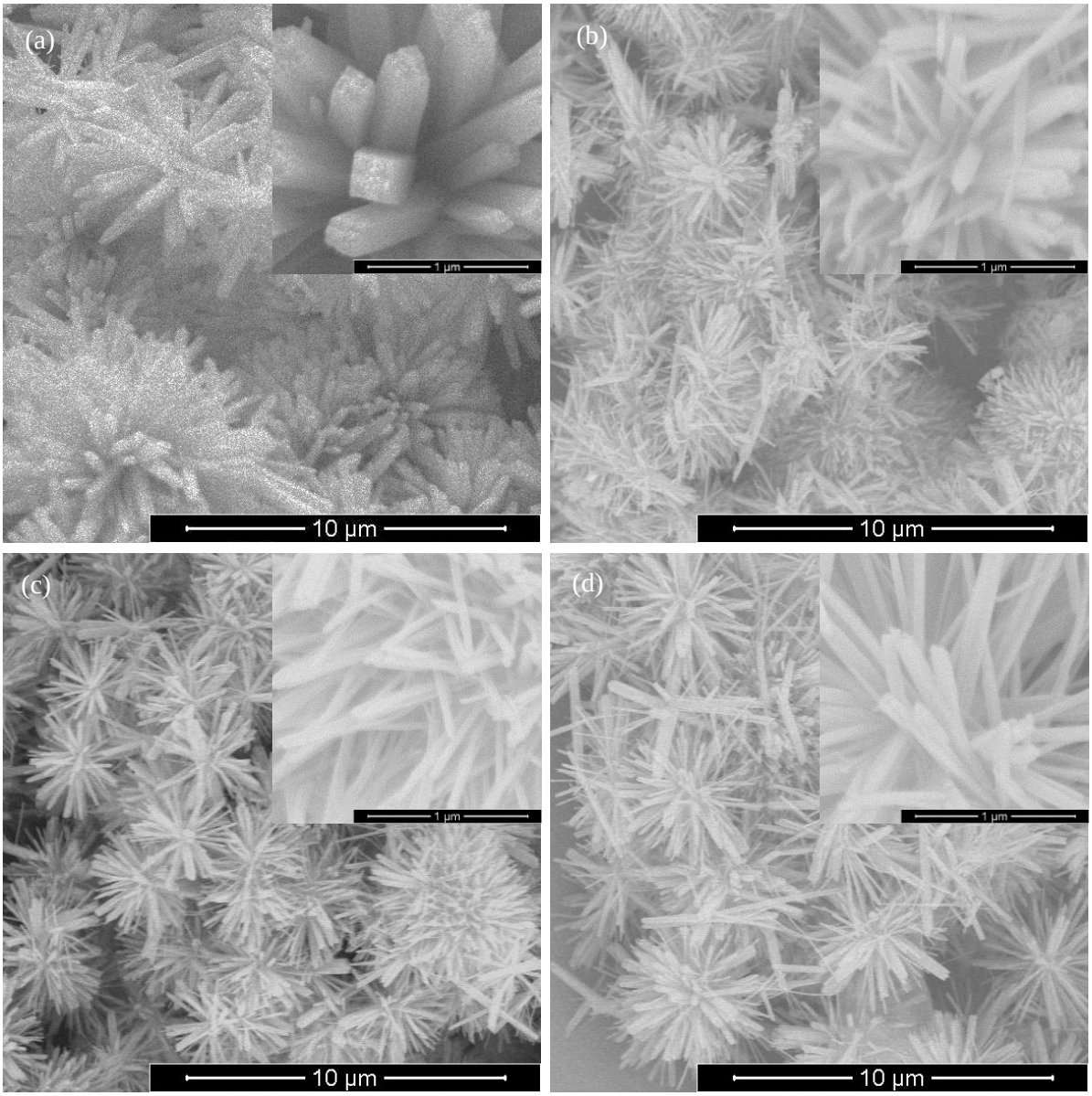

Figure 3 Secondary electron images of nano rosette TiO_2 hydrothermally synthesized at 170°C for 6 hours with addition of: (a) 0%; (b) 2.5%; (c) 5%; and (d) 10% v/v NaCl at low magnification (bar scale 10 µm). Inset is the image at high magnification (bar scale 1 µm)

The reaction steps for the nano formation without NaCl addition is given in Equation 1, whereas the nano formation with NaCl addition is given in Equation 2. Based on these reaction steps, the inhibition mechanism for this crystal growth is proposed as given schematically in Figure 3.

$$HCl_{(l)} + H_2O_{(l)} \Leftrightarrow H_3O^+_{(aq)} + Cl^-_{(aq)}$$

$$Ti\{OCH(CH_3)_2\}_{4(aq)} + 2H_3O^+_{(aq)} + 2Cl^-_{(aq)} \xrightarrow{\text{heat}} TiO_{2(s)} + 4(CH_3)_2CHOH_{(aq)} + 2H^+_{(aq)} + 2Cl^-_{(aq)} \quad (1)$$

$$HCl_{(l)} + H_2O_{(l)} + NaCl_{(aq)} \Leftrightarrow H_3O^+_{(aq)} + 2Cl^-_{(aq)} + Na^+_{(aq)}$$

$$Ti\{OCH(CH_3)_2\}_{4(aq)} + 2H_3O^+_{(aq)} + 4Cl^-_{(aq)} + 2Na^+_{(aq)} \xrightarrow{heat} TiO_{2(s)} + 4(CH_3)_2CHOH_{(aq)} + 2H^+_{(aq)} + 2Na^+_{(aq)} + 4Cl^-_{(aq)} \quad (2)$$

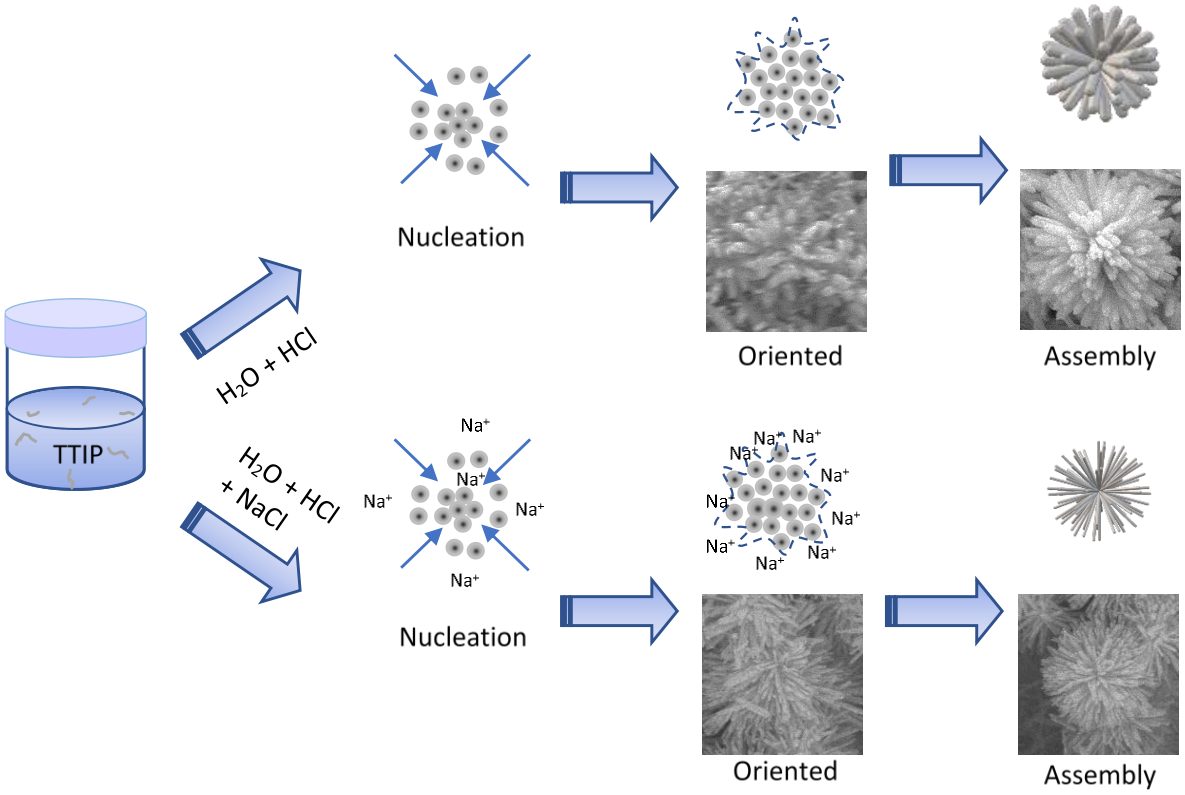

Figure 4 Schematic illustration of the 3D nano rosette rutile TiO_2 formation via different hydrothermal reactions with and without addition of NaCl

As can be seen in Figure 4, the steps for crystal formation are given according to the reaction pathways. For the hydrothermal reaction without NaCl addition, the deposition begins with a nucleation process in which the nuclei start to deposit on the substrate. With increasing hydrothermal reaction time, the acid environment prevents the occurrence of agglomeration and favors the homogeneous nucleation of tiny single crystals derived from the nuclei. As the reaction continued, the crystals come together, forming the early stage of rosette-shaped structure through oriented attachment while acid concentration acts as a structure-directing agent. At the last stage of the hydrothermal reaction, acid concentration helps to control the growth of different crystals' orientation to minimize their surface area and decrease their energy but without any interference, and thus the crystal can grow freely. At the same time, the assembly through self-organization of the petal-shaped structure occurs and the 3D hierarchical structure of the nano rosette rutile TiO_2 is obtained.

4. CONCLUSION

The effect of hydrothermal reaction time and NaCl addition on the characteristics of nano rosette TiO_2 crystal growth during hydrothermal reaction has been examined. With no addition of NaCl, the nano rosette forms at full growth indicated by high intensity of the crystal structure indexed to rutile $P4_2/mnm$ with lattice parameters of a = 4.557(6) Å and c = 2.940(5) Å. The cross-

sectional rosette petal grew up to 250 nm. On the contrary, with the addition of NaCl, the crystal growth during hydrothermal reaction could be controlled. In this work, with the addition of 2.5% v/v NaCl, the cross-sectional rosette size was only of about 50 nm, 80% smaller than that of the crystal grown with no NaCl addition.

5. ACKNOWLEDGEMENT

This work was funded by the Directorate of Research and Community Services (DRPM) Universitas Indonesia under Hibah PITTA No. 2504/UN2.R3.1/HKP.05.00/2018.

6. REFERENCES

Bai, J., Zhou, B., 2014. Titanium Dioxide Nanomaterials for Sensor Applications. *Chemical Review*, Volume 114, pp. 10131–10176

Banfield, J.F., Veblen, D.R., 1992. Conversion of Perovskite to Anatase and TiO_2 (B): A TEM Study and the Use of Fundamental Building Blocks for Understanding Relationships among the TiO_2 Minerals. *American Mineralogist*, Volume 77, pp. 545–557

Bu, J., Fang, J., Leow, W.R., Zheng, K., Chen, X., 2015. Single-Crystalline Rutile TiO_2 Nano-Flower Hierarchical Structures for Enhanced Photocatalytic Selective Oxidation from Amine to Imine. *RSC Advances*, Volume 5(126), pp. 103895–103900

Dahl, M., Liu, Y., Yin, Y., 2014. Composite Titanium Dioxide Nanomaterials. *Chemical Review*, Volume 114, pp. 9853–9889

Govindaraj, R., Santhosh, N., Pandian, M.S., Ramasamy, P., 2017. Synthesis of Nanocrystalline TiO_2 Nanorods via Hydrothermal Method: An Efficient Photoanode Material for Dye Sensitized Solar Cells. *Journal of Crystal Growth*, Volume 468, pp. 125–128

Govindasamy, G., Murugasen, P., Sagadevan, S., 2016. Investigations on the Synthesis, Optical and Electrical Properties of TiO_2 Thin Films by Chemical Bath Deposition (CBD) Method. *Materials Research*, Volume 19(2), pp. 413–419

Khan, J., Gu, J., Meng, Y., Chai, Z., He, S., Wu, Q., Tong, S., Ahmed, G., Mai, W., Wu, M., 2017. Anatase TiO_2 Single Crystal Hollow Nanoparticles: Their Facile Synthesis and High-Performance in Dye-sensitized Solar Cells. *CrystEngComm*, Volume 19, pp. 325–334

Liang, C., Wu, Z., Li, P., Fan, J., Zhang, Y., Shao, G., 2017. Chemical Bath Deposited Rutile TiO_2 Compact Layer Toward Efficient Planar Heterojunction Perovskite Solar Cells. *Applied Surface Science*, Volume 391(B), pp. 337–344

Liu, B., Aydil, E.S., 2009. Growth of Oriented Single-crystalline Rutile TiO_2 Nanorods on Transparent Conducting Substrates for Dye-sensitized Solar Cells. *Journal of American Chemical Society*, Volume 131, pp. 3985–3990

Longoni, G., Cabrera, R.L.P., Polizzi, S., D'Arienzo, M., Mari, C.M., Cui, Y., Ruffo, R., 2017. Shape-controlled TiO_2 Nanocrystals for Na-ion Battery Electrodes: The Role of Different Exposed Crystal Facets on the Electrochemical Properties. *Nano Letters*, Volume 17, pp. 992–1000

Ma, J., Ren, W., Zhao, J., Yang, H., 2017. Growth of TiO_2 Nanoflowers Photoanode for Dye-sensitized Solar Cells. *Journal of Alloys and Compounds*, Volume 692, pp. 1004–1009

Nakata, K., Fujishima, A., 2012. TiO_2 Photocatalysis: Design and Applications. *Journal of Photochemistry and Photobiology C: Photochemistry Reviews*, Volume 13(3), pp. 169–189

Patterson, A.L., 1939. The Scherrer Formula for X-Ray Particle Size Determination. *Physical Review*, Volume 56, pp. 978–982

Rahman, A., Nurjayadi, M., Wartilah, R., Kusrini, E., Prasetyanto, E.A., Degermenci, V., 2018. Enhanced Activity of TiO_2/Natural Zeolite Composite for Degradation of Methyl Orange under Visible Light Irradiation. *International Journal of Technology*, Volume 9(6), pp. 1159–1167

Saif, M., Aboul-Fotouh, S.M.K., El-Molla, S.A., Ibrahim, M.M., Ismail, L.F.M., 2012. Improvement of the Structural, Morphology, and Optical Properties of TiO_2 for Solar Treatment of Industrial Wastewater. *Journal of Nanoparticle Research*, Volume 14(1227), pp. 101–111

Sofyan, N., Ridhova, A., Yuwono, A.H., Udhiarto, A., 2017. Fabrication of Solar Cells with TiO_2 Nanoparticles Sensitized using Natural Dye Extracted from Mangosteen Pericarps. *International Journal of Technology*, Volume 8(7), pp. 1229–1238

Sofyan, N., Ridhova, A., Yuwono, A.H., Udhiarto, A., Fergus, J.W., 2019. Synthesis of TiO_2 Nanoparticles at Low Hydrothermal Temperature and Its Performance for DSSC Sensitized using Natural Dye Extracted from Melastoma Malabathricum L. Seeds. *International Journal of Energy Research*, Volume 43(11), pp. 5959–5968

Sofyan, N., Ridhova, A., Yuwono, A.H., Wu, J., 2018. Characteristics of Nano Rosette TiO_2 Hydrothermally Grown on a Glass Substrate at Different Reaction Times and Acid Concentrations. *International Journal of Technology*, Volume 9(6), pp. 1196–1204

Xiao, G., Shi, C., Li, L., Zhang, Z., Ma, C., Lv, K., 2017. A 200-nm length TiO_2 Nanorod Array with a Diameter of 13 nm and Areal Density of 1100 μm -2 for Efficient Perovskite Solar cells. *Ceramics International*, Volume 43(15), pp. 12534–12539

Xie, J., Lü, X., Liu, J., Shu, H., 2009. Brookite Titania Photocatalytic Nanomaterials: Synthesis, Properties, and Applications. *Pure and Applied Chemistry*, Volume 81(12), pp. 2407–2415

Zhang, H., Chen, W.-G., Li, Y.-Q., Jin, L.-F., Cui, F., Song, Z.-H., 2018. 3D Flower-Like NiO Hierarchical Structures Assembled With Size-controllable 1D Blocking Units: Gas Sensing Performances Towards Acetylene. *Frontiers in chemistry*, Volume 6(472), pp. 1–6

Zhong, D., Jiang, Q., Huang, B., Zhang, W.-H., Li, C., 2015. Synthesis and Characterization of Anatase TiO_2 Nanosheet Arrays on FTO Substrate. *Journal of Energy Chemistry*, Volume 24, pp. 626–631

Zhou, J., Tian, G., Chen, Y., Wang, J.-Q., Cao, X., Shi, Y., Pan, K., Fu, H., 2013. Synthesis of Hierarchical TiO_2 Nanoflower with Anatase-rutile Heterojunction as Ag Support for Efficient Visible-light Photocatalytic Activity. *Dalton Transactions*, Volume 42(31), pp. 11242–11251

Zhu, Z., Lin, S.-J., Wu, C.-H., Wu, R.-J., 2018. Synthesis of TiO_2 Nanowires for Rapid NO_2 Detection. *Sensors and Actuators A*, Volume 272, pp. 288–294